26th INTERNATIONAL CONGRESS ON SOUND AND VIBRATION
7-11 July 2019, Montreal

REFLECTION FROM A NON-UNIFORM ACOUSTIC WAVEGUIDE WITH FITTED RIGID RINGS USING A TRANSFER FUNCTION METHOD

Angelis Karlos and Stephen J. Elliott
Institute of Sound and Vibration Research, University of Southampton, Southampton, SO17 1BJ, United Kingdom
email: A.Karlos@soton.ac.uk

An acoustic waveguide consisting of a cylindrical tube with fitted thin rigid rings whose inner radius decreases appropriately causes incident acoustic waves to slow down, resulting in considerable absorption in the cavities between the rings. The absorption becomes greater towards the end of the waveguide, where the wave speed becomes very small and the waves are spatially concentrated. Such a system demonstrates the so-called 'Acoustic Black Hole' effect. In this paper, the reflection coefficient of an acoustic waveguide whose ring inner radius has either a linear or a quadratic profile is calculated, using a Transfer Function method. A Transmission Line model is also used, which forms a low-frequency approximation to the Transfer Function method. Different geometrical assumptions for the cavity between two consecutive rings and for the core of the waveguide are considered for both methods. The results are compared with experimental ones from the literature. The numerical results predict the general characteristics of the reflection coefficient. For the linear case, the fluctuations of the reflection coefficient are also predicted over part of the spectrum.

Keywords: Acoustic Black Hole, Transfer Function

1. Introduction

The concept of absorption of flexural waves on a plate with a termination of a tapered power-law thickness of order equal to or greater than two was introduced by Mironov in [1]. A similar idea was proposed for acoustic waves by Mironov and Pislyakov in [2], where thin rigid rings of decreasing inner radius were fitted inside a tube terminated at a rigid wall. An analytical model was presented, where the compliance of the discrete cavities between consecutive rings was approximated by a continuous equivalent wall admittance. It was shown that for the case of such an acoustic waveguide, the variation of the inner radius of the rings can be of order one, that is linear, or higher. It was theoretically predicted in [2] that, in a waveguide with inner-radius variation of order one, that is, linear, or higher, an incident acoustic wave slows down theoretically to zero propagation velocity at the end of the waveguide, where the equivalent continuous inner radius of the vanishes. In practice, however, the last ring always has a non-zero inner-radius, so that reflection takes place at the termination of the waveguide.

A numerical approach using Transmission Matrices was presented in [3], and results for the reflection coefficient were compared with those from the analytical method presented in [2], both for a linear and a quadratic ring inner-radius variation. The variation of the reflection coefficient with respect to the variation of several parameters of the model was also presented. The reflection coefficient for waveguides with both linear and quadratic ring inner-radius variations was measured experimentally, using an impedance tube, by Azbaid El Ouahabi et al. in [4] and [5].

In this paper, a method based on the Transfer Function of the acoustic admittance is presented. This method is equivalent to the Transmission Matrix method presented in [3] when the latter is used to calculate the input impedance or the reflection coefficient, since this does not require the knowledge of the acoustic pressure and volume velocity, which are both explicitly calculated with the Transmission Matrix method. A Transmission Line model is also presented, which forms an approximation of the initial Transfer Function method when the inter-ring distances are small compared to the wavelength. Two different geometrical approaches are considered for the representation of the inter-ring cavities and of the core of the waveguide between two consecutive rings, namely, a cylindrical and a conical one. Results for both linear and quadratic waveguides with the Transfer Function and the Transmission Line method, and with different modelling geometrical shapes for the cores and cavities, are compared to each other, as well as against the experimental results presented in [5]. The similarities and discrepancies between the numerical and experimental results are discussed.

2. Methods

A graphic representation of a longitudinal cross section of a non-uniform waveguide consisting of a cylindrical tube with fitted rings of varying inner radius is shown in Fig. 1. The non-uniform waveguide forms a termination to a cylindrical tube of slightly smaller radius, in accordance with the experimental setup presented in [5].

A numerical method using Transmission Matrices for calculating the reflection coefficient of such a waveguide was presented in [3]. This method calculates the input impedance and, from this, the reflection coefficient by calculating the acoustic pressure and volume velocity at the input boundary. A similar but simpler method can be followed if only the input impedance and the reflection coefficient are sought for. Namely, instead of using Transmission Matrices, the Transfer Functions of the impedance or, equivalently, the admittance can be used. Similarly to [3], the waveguide is divided in longitudinal elements, each of which starts from the left, or input, boundary of a ring and finishes at the input boundary of the next ring, as depicted in Fig. 2. The method provides the input admittance of the element from a known input admittance of the next element. Thus, starting from a known admittance at the termination of the waveguide, in this case, where the waveguide has a rigid termination, $Y_{end} = 0$, as shown in Fig. 1, the input admittance of the whole waveguide can be found, by iteratively calculating the input admittance of each element of the waveguide, starting from the last, that is, the rightmost one. The Transfer Function method, like the Transmission Matrix method, assumes plane wave propagation and is therefore limited by the cut-off frequency of the first higher-order radial mode. It also does not take into account any nearfield pressures at the end of the rings, including any end effects or interaction between adjacent rings.

Three effects need to be accounted for in calculating the input admittance of a given element. These are the compliance of the cavities between two consecutive rings, corresponding to the lined region in Fig. 2, the propagation of the acoustic wave in the core of the waveguide between the two rings, and the propagation of the wave in the thin region of the ring [3]. The parallel combination of the input admittance of the $(n+1)$-th element with the admittance due to the compressibility of the cavity is given by

$$\tilde{Y}_{c,n} = Y_{c,n} + Y_{n+1}, \tag{1}$$

where $Y_{c,n}$ is the admittance of the n-th cavity and Y_{n+1} is the input admittance of the $(n+1)$-th element.

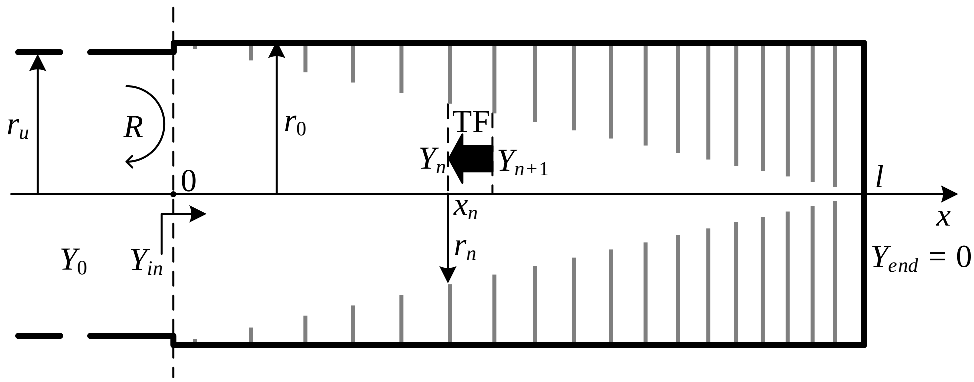

Figure 1: Schematic representation of a longitudinal cross section of a waveguide of length l, which consists of a rigidly terminated cylindrical tube of radius r_0 with 18 thin rigid rings of linearly varying inner radius. The non-uniform waveguide forms a termination to a semi-infinite cylindrical tube of slightly smaller radius, r_u, in accordance with the experimental setup in [5]. The input admittance, Y_{in}, the termination admittance, Y_{end}, and the intermediate admittances, Y_n and Y_{n+1}, of the n-th and $(n+1)$-th ring, respectively, are shown, along with the longitudinal position, x_n, and the inner radius, r_n, of the n-th ring. The reflection coefficient at the connection of the uniform and non-uniform parts is denoted by R. The calculation of the admittance at the input position of a ring of arbitrary order from the admittance at the input position of the next ring is represented by a thick arrow and labelled as TF, which stands for Transfer Function.

The admittance of the cavity can be approximated by a lumped admittance [6]

$$Y_{c,n} = \mathrm{i}ky_0V_n, \tag{2}$$

where i is the imaginary unit, $k = \omega/c$ is the wavenumber, where ω is the angular frequency and c is the speed of sound, $y_0 = (\rho c_0)^{-1}$ is the characteristic specific acoustic admittance of air, where c_0 is the lossless speed of sound, and V_n is the volume of the cavity. In Eq. (2), it is assumed that the radial dimensions of the cavity are much smaller than the wavelength [3]. Losses in the system are included by an imaginary part in the speed of sound, $c = c_0(1 + \mathrm{i}\mu)$, where μ is a positive constant.

The cavity region can be considered as either the difference of two cylinders or the difference of a cylinder and a truncated cone, corresponding to the two different lined regions on Fig. 2. Therefore, the volume of the n-th cavity can have either of the two forms

$$V_{n,cyl} = \pi h_{c,n}\left(r_0^2 - r_n^2\right),\ V_{n,con} = \pi h_{c,n}\left[r_0^2 - \frac{1}{3}\left(r_n^2 + r_{n+1}^2 + r_nr_{n+1}\right)\right], \tag{3}$$

where r_0 is the radius of the tube in which the rings are fitted and r_n is the inner radius of the n-th ring.

Accordingly, the core of the element can be modelled as either a cylinder or a truncated cone. This leads to two different forms for the Transfer Function of the admittance accounting for the propagation along the core of the n-th element [6],

$$\tilde{Y}_{n,cyl} = S_ny_0\frac{\mathrm{i}S_ny_0\sin(kh_{c,n}) + \tilde{Y}_{c,n}\cos(kh_{c,n})}{S_ny_0\cos(kh_{c,n}) + \mathrm{i}\tilde{Y}_{c,n}\sin(kh_{c,n})}, \tag{4}$$

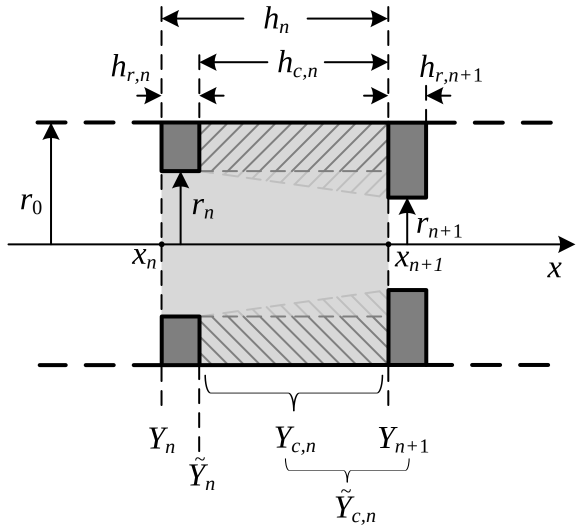

Figure 2: Detailed schematic of an element of the waveguide, showing the difference between the cylindrical and conical assumed geometries, comprising the region which starts from the input boundary of the n-th ring, located at x_n, and finishes at the input boundary of the $(n+1)$-th ring, located at x_{n+1}. The length of the element region is h_n, which consists of the thickness of the n-th ring, $h_{r,n}$, and the length between the n-th and $(n+1)$-th rings, $h_{c,n}$. The admittances at the inputs of the n-th and $(n+1)$-th rings, Y_n and Y_{n+1}, respectively, are shown, along with admittances involved in intermediate calculations, which are explained in the text.

where $S_n = \pi r_n^2$ is the cross-sectional area of the region of propagation, and [7]

$$\tilde{Y}_{n,con} = S_n y_0 \frac{S_{n+1} y_0 \sin(kh_{c,n} + \theta_{n,1} - \theta_{n,2}) - \mathrm{i}\tilde{Y}_{c,n} \sin(kh_{c,n} + \theta_{n,1}) \sin\theta_{n,2}}{\mathrm{i}S_{n+1} y_0 \sin(kh_{c,n} - \theta_{n,2}) \sin\theta_{n,1} + \tilde{Y}_{c,n} \sin(kh_{c,n}) \sin\theta_{n,1} \sin\theta_{n,2}}, \tag{5}$$

where $\theta_{n,1} = \tan^{-1}(kh_{c,n} r_n / d_n)$, $\theta_{n,2} = \tan^{-1}(kh_{c,n} r_{n+1} / d_n)$ and $d_n = r_{n+1} - r_n$.

The last effect that needs to be accounted for is the propagation along the thin cylindrical region of the ring, giving the impedance at the input of the n-th element as

$$Y_n = S_n y_0 \frac{\mathrm{i}S_n y_0 \sin(kh_{r,n}) + \tilde{Y}_n \cos(kh_{r,n})}{S_n y_0 \cos(kh_{r,n}) + \mathrm{i}\tilde{Y}_n \sin(kh_{r,n})}. \tag{6}$$

The reflection coefficient can then be calculated by [8]

$$R = \frac{Y_0 - Y_{in}}{Y_0 + Y_{in}}, \tag{7}$$

where Y_0 is the characteristic acoustic admittance of the cylindrical tube, given by $Y_0 = y_0 S_0$. In the presented set of equations, either the combination of the first of Eqs. (3) with Eq. (4) or the combination of the second of Eqs. (3) with Eq. (4) has to be used, corresponding to the cylindrical and the conical approach, respectively, for the cavity and the core of an element of the waveguide.

A Transmission Line model consisting of lumped parameters can also be used. It can be shown that the Transmission Line model is equivalent to the Transfer Function method when the distances between consecutive rings are much smaller than the wavelength. Therefore, the Transmission Line forms a low frequency approximation to the Transfer Function method.

The shunt admittance of a segment between two rings is given by

$$Y_{C,n} = \mathrm{i}ky_0 \left(h_{c,n} S_0 + h_{r,n} S_n \right). \tag{8}$$

For the calculation of the series admittance due to the inertance of the fluid, two regions are considered, namely, the thin cylindrical region of the ring and the core region between the two rings, the latter of which can be either cylindrical or conical, as explained above. For the cylindrical approach, the series admittance is given by

$$Y_{L,n,cyl} = \frac{S_n y_0}{\mathrm{i}kh_n}, \tag{9}$$

whereas, for the conical approach, the series combination of the inertances of the two regions gives

$$Y_{L,n,con} = \frac{\pi r_n^2 r_{n+1} y_0}{\mathrm{i}k(r_n h_{c,n} + r_{n+1} h_{r,n})}. \tag{10}$$

The admittance of the n-th segment is given by

$$Y_n = \frac{Y_{C,n} + Y_{n+1}}{Y_{L,n} + Y_{C,n} + Y_{n+1}} Y_{L,n}. \tag{11}$$

The reflection coefficient can then be calculated with Eq. (7).

3. Results and Discussion

In this analysis, both a waveguide with linear and one with quadratic ring inner-radius variation are considered. Initially, the Transmission Line method is assessed by comparing results with corresponding ones from the Transfer Function method. Subsequently, results from the Transfer Function method are compared with experimental ones from Azbaid El Ouahabi et al. [5]. Therefore, the geometrical properties of the system, shown in Table 1, are in accordance with [5]. The upper limit of the considered spectrum is defined by the plane wave assumption, and it is calculated by $f_u = 0.293c_0/r_0$ [7], giving an upper limit of around 874 Hz. A loss parameter with a value of $\mu = 0.05$ has been used in all the simulations, to provide good matching with the experimental results.

The modulus of the reflection coefficient calculated with the Transfer Function and Transmission Line methods, using either the cylindrical or the conical approach, is shown in Figs. 3a and 3b, for linear and quadratic ring inner-radius variation, respectively. It can be seen that the results from the two geometrical approaches diverge from each other as frequency increases, particularly in terms of the frequencies of the minima in the responses. The Transmission Line results appear to match well with the ones from The Transfer Function method at lower frequencies. However as frequency increases, the Transmission Line method predicts smaller fluctuations in the reflection coefficient. This can be linked to the fact that, at lower frequencies, the dimensions of each element are relatively smaller compared to the wavelength than they are at higher frequencies, and, therefore, the approximation of the Transmission Line is more valid there. The pronounced dip in the reflection coefficient at about 155 Hz, based on the conical approach, appears to be due to a half-wavelength resonance between the input of the waveguide and some position close to the end, which would imply a pressure release at that position.

Geometrical property	Value	Geometrical property	Value (Linear)	Value (Quadratic)
Radius of tube with rings (r_0)	115 mm	Number of rings (N)	18	15
Ring thickness (h_r)	2 mm	Position of first ring (x_1)	6 mm	
Length of tube with rings (l)	255 mm	Distance between n-th and $(n+1)$-th ring ($h_{c,n}$)	$(21-n)$ mm, $1 \leq n \leq N$	
Radius of uniform tube (r_u)	112.5 mm	Position of n-th ring (x_n)	$x_1 + \sum_{m=1}^{n-1}(h_r + h_{c,m})$, $2 \leq n \leq N$	
		Distance between last ring and end	9 mm	30 mm
		Ring inner radius (r_n)	$r_0(1 - x_n/l)$	$r_0(1 - x_n/l)^2$

Table 1: Geometrical properties of the system, based on [5].

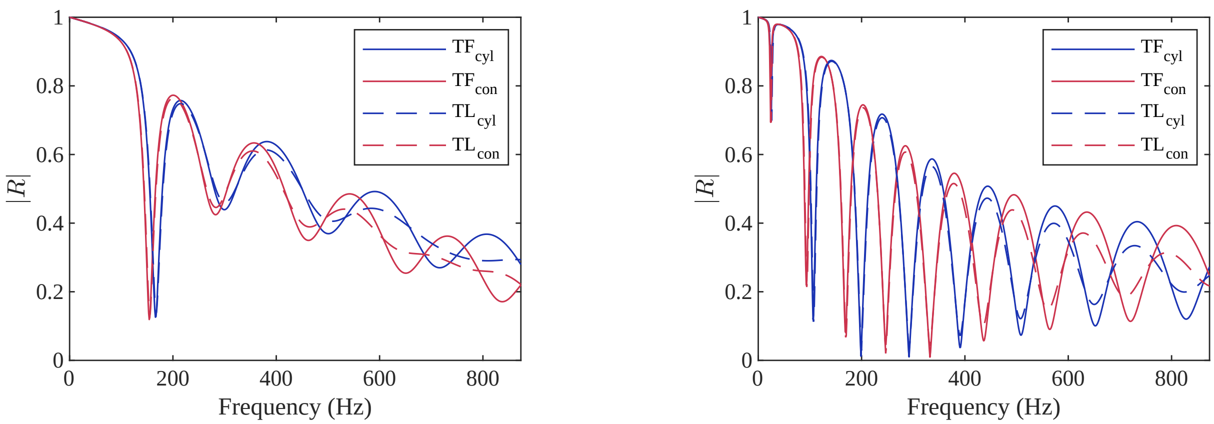

(a) (b)

Figure 3: Modulus of the reflection coefficient calculated with the Transfer Function and Transmission Line methods, using the cylindrical and the conical approach, for (a) linear and (b) quadratic inner-radius variation. The geometrical properties of the waveguides are presented in Table 1.

Comparing results from the two methods using a similar geometry but with 40 rings, which are equally spaced, gives a much better correspondence, as can be seen in Figs. 4a and 4b, for the linear and quadratic cases, respectively. This is due to the fact that a larger number of rings leads to a larger number of elements, which, in turn, leads to a smaller element length. Therefore, the element length becomes smaller compared to the waveguide as the number of rings increases, which renders the Transmission Line approximation more accurate.

Due to the considerable deviation of the Transmission Line results from the Transfer Function ones at higher frequencies for the systems used in the experiments in [5], only the Transfer Function results are compared with the experimental ones. It would also appear that the results with the conical assumption are the most accurate representation of the experimental results,and so they also selected. The moduli of the reflection coefficient taken from the experimental results in [5] along with the reflection coefficient calculated with the cylindrical and conical approaches of the Transfer Function method, are plotted in Figs. 5a and 5b, for the linear and quadratic cases, respectively. It should be noted that the measured response is also unreliable below about 114 Hz, due to limitations in the experimental setup, as explained in [5]. The value for the loss parameter $\mu = 0.05$ has been chosen to provide good correspondence of

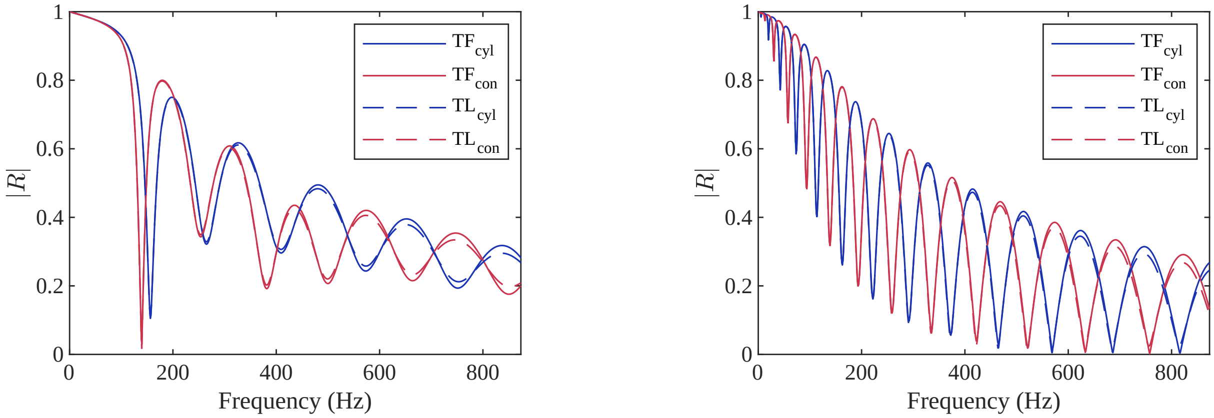

(a) (b)

Figure 4: Modulus of the reflection coefficient calculated with the Transfer Function and Transmission Line methods, using the cylindrical and the conical approach, for (a) linear and (b) quadratic inner-radius variation. The length and radii of the uniform and non-uniform parts of the waveguide are those given in Table 1, but 40 equally spaced rings of a thickness of 1 mm are used for both the linear and quadratic waveguides.

the numerical results with the experimental ones for the general level of the modulus of the reflection coefficient at the middle region of the considered spectrum.

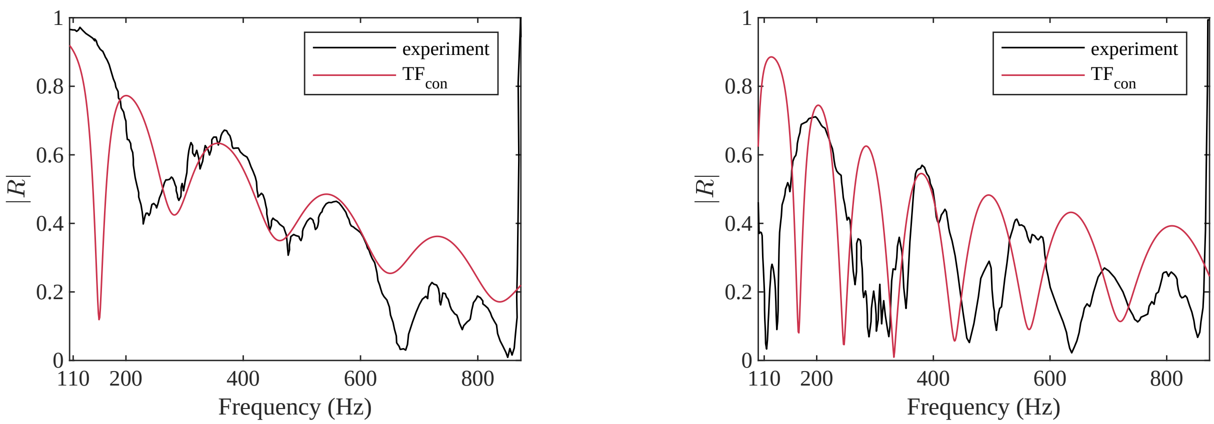

(a) (b)

Figure 5: Modulus of the reflection coefficient from the experiments by Azbaid El Ouahabi et al. taken from [5],compared to that calculated with the Transfer Function method, using the conical approach, for (a) linear and (b) quadratic inner-radius variation.

In the case of linear ring inner-radius variation, the modulus of the reflection coefficient with the conical approach appears to match relatively well at the middle region of the considered spectrum with that obtained experimentally, that is, between about 300 and 600 Hz. Even at higher frequencies, the frequencies of the two main dips of the experimentally measured reflection coefficient, one around 670 Hz and one around 850 Hz, are relatively well predicted, even though the level of the reflection coefficient is higher in the numerical results. If the loss parameter is chosen to be greater, the correspondence of the level of the modulus of the reflection coefficient improves at higher frequencies but it deteriorates at lower frequencies. The results from the cylindrical approach, not plotted, give worse results, especially at higher frequencies. This could be justified by the fact that the conical approach would be expected to form a more accurate geometrical representation of the cavities and cores of the waveguide. Additional simulations showed that the different representation of the core causes the main difference between the two geometrical approaches, while the assumed shape of the cavity is not so important. The predicted dip in the reflection coefficient at about 155 Hz is not observed in the experimental results.

For quadratic ring inner-radius variation, the Transfer Function results predict the general trend of the level of the modulus of the reflection coefficient well with the chosen value for μ. The distances between consecutive dips in the modulus of the reflection coefficient are of similar width as the experimental ones. However, the details of the Transfer Function results do not match well with the experimental ones, that is, they do not follow the fluctuations, over any extended bandwidth.

4. Conclusions

A Transfer Function method has been presented for the calculation of the reflection coefficient of an acoustic waveguide with fitted thin rigid rings, following one of two geometrical approaches. The assumption of a conical core between the rings is shown to give significantly different results from previous assumptions of cylindrical geometry, and appears to be a more accurate representation of the true geometry. A Transmission Line model has also been presented, which forms a low-frequency approximation of the Transfer Function Method. The results from the Transfer Function method were compared with experimental ones from the literature [5]. It was found that for the case of linear ring inner-radius variation, the conical approach can give a fairly good match with the experimental results in the middle frequency range of the considered spectrum. For the case of quadratic ring inner-radius variation, the numerical results are limited to predicting the general characteristics of the experimental response.

REFERENCES

1. Mironov, M. A. Propagation of a flexural wave in a plate whose thickness decreases smoothly to zero in a finite interval, *Soviet Physics: Acoustics*, **34** (3), 318–319, (1988).

2. Mironov, M. A. and Pislyakov, V. V. One-dimensional acoustic waves in retarding structures with propagation velocity tending to zero, *Acoustical Physics*, **48** (3), 347–352, (2002).

3. Guasch, O., Arnela, M. and Sánchez-Martín, P. Transfer matrices to characterize linear and quadratic acoustic black holes in duct terminations, *Journal of Sound and Vibration*, **395**, 65–79, (2017).

4. Azbaid El Ouahabi, A., Krylov, V. V. and O'Boy, D. J. Experimental investigation of the acoustic black hole for sound absorption in air, *Proceedings of the 22nd International Congress of Sound and Vibration*, (2015).

5. Azbaid El-Ouahabi, A., Krylov, V. V. and O'Boy, D. J. Investigation of the acoustic black hole termination for sound waves propagating in cylindrical waveguides, *44th International Congress and Exposition on Noise Control Engineering*, (2015).

6. Olson, H. F., *Acoustical Engineering*, D. Van Nostrand Company, Inc., USA (1957).

7. Fletcher, N. H. and Rossing, T. D., *The Physics of Musical Instruments*, Springer-Verlag, New York, 2nd edn. (1998).

8. Blackstock, D. T., *Fundamentals of Physical Acoustics*, Wiley and Sons Ltd, New York (2000).